

AugInsert: Learning Robust Visual-Force Policies via Data Augmentation for Object Assembly Tasks

Ryan Diaz¹, Adam Imdieke¹, Vivek Veeriah², Karthik Desingh¹

¹University of Minnesota, ²Google DeepMind

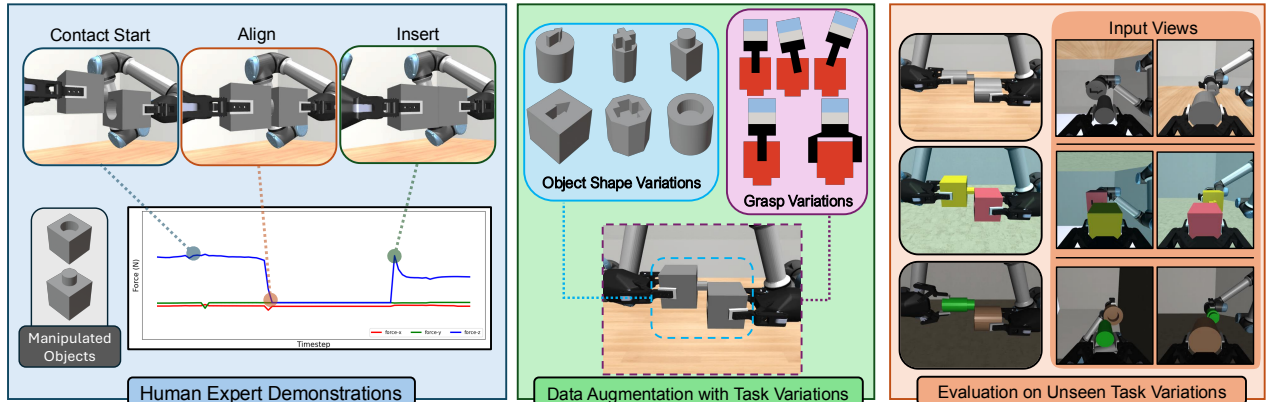


Fig. 1: AugInsert is a data collection and policy evaluation pipeline aimed towards analyzing the robustness of a multisensory (vision, force-torque, and proprioception) model with respect to different observation level task-variations in object shape, grasp pose, and visual environmental appearance. Our framework introduces task variations to a dataset of human-collected demonstrations through a system of online data augmentation.

Abstract—This paper primarily focuses on learning robust visual-force observation encoders to imitate policies in the context of object assembly tasks. Specifically, we focus on the *contact phase* of assembly task where both objects (peg and hole) have made contact and the task lies in finding contact-rich maneuvers to complete the assembly. Moreover, we aim to learn contact-rich manipulation policies with multisensory inputs on limited human demonstration data expanded via online data augmentation. We develop a simulation environment with a dual-arm robot manipulator to evaluate the effect of augmented expert demonstration data. We evaluate the performance of our model trained on an increasing number of augmentations per demonstration and at the same time evaluate the performance with respect to unseen task variations: *grasp pose, peg/hole shape, object body shape, scene appearance, camera pose, and force-torque/proprioception noise*. We show that our proposed data augmentation method helps in learning a multisensory manipulation policy that is robust to unseen variations, particularly physical variations such as *grasp pose*. For additional qualitative results and ablation studies, we refer to the project webpage <https://bit.ly/47skWXH>.

I. INTRODUCTION

Peg-in-hole assembly tasks are representative of many everyday tasks involving contact-rich manipulation, where objects remain in contact throughout the process. Consider tasks such as capping a bottle, plugging in a cable, or inserting a K-cup pod into a coffee machine. These tasks typically involve multiple phases: a *pick-up phase* where the objects (e.g., cap and bottle) are grasped and picked up by the grippers; an *orienting phase*, where the objects are maneuvered into a desired relative pose before contact; and a *contact phase*, where the objects are in contact, and appropriate forces are applied to complete the task (e.g.,

screwing the cap onto the bottle, fully inserting the plug). While the *contact phase* may seem trivial to perform for humans, it poses significant challenges for robots—especially those meant to operate in household contexts—to learn from data due to several factors: a) contact-rich manipulation tasks are difficult for humans to demonstrate in order to facilitate large scale data collection for learning policies from demonstration, b) these tasks require multisensory observations (visual and tactile) and robust encoding methods to extract meaningful representations for policy learning [1]–[4], and c) humans can easily generalize these tasks to novel scenarios (e.g. varying object shapes and geometries), but such generalization is highly challenging for robot learning models while maintaining the robustness required [5], [6].

In this paper, we address these challenges by proposing a multisensory observation encoding and policy learning framework, leveraging data augmentation on limited human demonstrations to train contact-rich manipulation policies for an assembly task that generalizes to unseen task variations. Our pipeline processes multiple camera views and force-torque readings from a dual-arm setup. We also make use of a multisensory data augmentation method via trajectory replay that can introduce both sensor-specific (camera and force-torque sensor) variations as well as physical factors such as manipulated object shape, peg and hole geometries, and grasp pose variations that affect the sensing modalities. In this way, we can expand small expert datasets to learn robust manipulation policies that can handle a wide variety of environmental conditions.

To analyze the robustness of our model with respect to specific observation-level task variations and understand the

effect of our data augmentation method, we develop an experimental setup in the MuJoCo [7] simulation environment with a dual-arm robot that can manipulate objects with peg and hole geometries to complete the assembly task. Our experiments show that certain variations, such as *Grasp Pose* variations, cause large drops in success rate for our task and so should be included in training data through data augmentation in order to ensure robustness to these variations. Additionally, we conduct ablation studies to understand how each sensory modality in the multisensory setup affects the performance of the contact-rich assembly task. These studies also help identify the specific variations impacted by each modality. We observe that touch provides the most relevant information for the task and supports model robustness; visual input, on the other hand, has the least significant impact on generalization ability while also being susceptible to many of our task variations. We provide an extensive discussion of these results in the following sections.

The main contributions of our work are:

- A dual-arm object assembly task formulation and a simulation environment that allows for independent application of 6 types of task variations that involve 54 different types of peg and hole objects.
- A data augmentation pipeline integrated with the simulation environment that can generate new observations for training using a set of provided expert demonstrations through trajectory replay.
- An extensive set of experiments to understand the effect of data augmentation and evaluate the robustness of specific sensing modes against observation-level task variations.

II. RELATED WORK

A. Multisensory Contact-Rich Manipulation

Multisensory contact-rich manipulation in the form of peg-in-hole insertion using vision and force-torque data has been widely studied. Lee et al. [1] developed a self-supervised learning method to learn a multisensory representation using vision and force-torque. In their follow up work [8] they add a reconstruction and latent distance objective to their self-supervision framework to mitigate the effects of possible sensor corruption. More recently, Spector et al. [3], [4] developed a multiview and multisensory system for localizing and performing realistic insertion tasks, Chen et al. [2] used a transformer [9] encoder for vision and force-torque inputs to learn a higher-quality representation, and Kohler et al. [10] leveraged symmetry in the peg-in-hole task by using equivariant networks to improve sample efficiency. Although these works can achieve efficient peg-in-hole assembly, their generalization studies are limited in scope when evaluating robustness to both physical and sensory task variations.

B. Evaluating Generalization Abilities of Learned Policies

Generalization is difficult to define in robot manipulation policy learning as there are several factors in the robot's environment that could vary from training phase to the evaluation phase. There have been recent efforts to perform in-depth analyses of the generalization abilities of visuomotor

robotic policies by decomposing task environment variations into individual variation “factors” [5], [6], [11], [12]. We aim to bring this type of analysis to the multisensory domain by introducing a set of variation factors that perturb force-torque and proprioceptive inputs in addition to image inputs.

C. Extrapolating Human Trajectories for Imitation Learning

Imitation learning can be a powerful method for learning complex tasks in robotics, but it can be challenging to collect large enough demonstration datasets for learning effective policies. Recent works address this problem by extrapolating a small dataset of human demonstrations; Mandlekar et al. [13] generated new trajectories by decomposing task demonstrations into object-centric subtasks, and Jia et al. [14] used different point cloud projections as new observations to simulate new transitions within a demonstration. Focusing more on robotic assembly, Ankile et al. [15] annotated expert trajectories with “bottleneck” states off of which perturbations and their corresponding corrective actions could be automatically generated. These works somewhat resemble our trajectory replay method for online augmentation, but they are more suited for long-horizon tasks that do not necessarily focus on precision.

III. TASK SETUP

A. Assembly Task Definition

Our experimental setup consists of a dual-arm robot manipulator with a multisensory configuration, featuring two force-torque (F/T) sensors and two RGB cameras attached to its wrists. The robot is tasked with performing an insertion assembly, where one arm's gripper holds a peg-shaped object and inserts it into a hole-shaped object held by the other arm's gripper. Since our focus is on the contact phase of the assembly, the objects are already in contact at the start of the task.

The objective of the robot learning framework is to execute the assembly task without explicit information about the object geometries or peg-and-hole shapes, while maintaining robustness to various task variations. We take the behavior cloning approach where expert demonstrations are used to clone the contact-rich manipulation policy to perform the assembly.

B. Task Initialization

The task is initialized with the peg and hole offset within a range of [1.5cm, 3.0cm] along both the X and Y axes relative to the object coordinate frame (perpendicular to the direction of insertion). Our setup ensures that while the arm holding the peg moves, the other arm remains compliant, applying a constant force until the peg and hole are aligned. To define a successful task rollout, we consider position coordinates $\mathbf{p} = (x_p, y_p, z_p)$ for the peg object and $\mathbf{h} = (x_h, y_h, z_h)$ for the hole object in the global coordinate frame. We set thresholds $\mathbf{d} = (d_x, d_y, d_z)$ such that during a successful insertion, $|\mathbf{p}_i - \mathbf{h}_i| < \mathbf{d}_i$ for all axes $i \in \{x, y, z\}$.

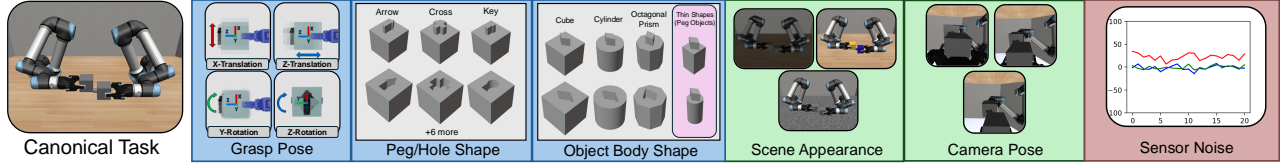


Fig. 2: A visualization of each of the task variations used in our environment setup. We differentiate between physical task variations (in blue) and sensor-based task variations that target vision (green) and force-torque/proprioception (red).

C. Task Variations

To evaluate the robustness of our trained models, we design a set of observation-level task variations which alter the distribution of incoming observations while preserving the underlying task. In total, there are six variations that are part of the experiments (see Fig. 2 for sample visualizations of these variations):

- 1) **Peg and Hole Shape:** There are 9 possible peg and hole shapes, with each peg and hole sharing the same shape and allowing for a tolerance to ensure insertion compatibility.
- 2) **Object Body Shape:** There are 3 possible object body shapes, and the peg and hole in a given pair may not share the same shape. Additionally, we create thinner versions of the peg to introduce variability, resulting in 6 total peg and hole object pairs.
- 3) **Grasp Pose:** Our grasp pose variation follows the approach in [16], which provides a more detailed overview.
- 4) **Scene Appearance:** This category encompasses variations in lighting, floor texture, and object color.
- 5) **Camera Pose:** We vary the position and orientation of the wrist cameras between demonstrations, while keeping them constant within each demonstration.
- 6) **Sensor Noise:** We add zero-mean Gaussian noise to low-dimensional measurements, with standard deviations set to approximately 5% of the maximum measurement for force-torque and 4% of the maximum task-initialized offset for proprioception.

Canonical Task Setup: We define a “canonical” task setup which represents an environment without any task variations applied. For discrete task variations, we choose the key peg and hole shape, cube object body shape, and light-wood floor texture in our canonical setup.

IV. METHODOLOGY

A. Imitation Learning Framework

Observation and Action Spaces: In our task, the observation space is defined as a composition of four modality spaces, $\mathcal{O} = \mathcal{I}_{left} \times \mathcal{I}_{right} \times \mathcal{T} \times \mathcal{S}$. The image spaces, $\mathcal{I}_{left} \subseteq \mathbb{R}^{84 \times 84 \times 3}$ and $\mathcal{I}_{right} \subseteq \mathbb{R}^{84 \times 84 \times 3}$, represent 84×84 RGB wrist views from the left and right arms. The tactile space, $\mathcal{T} \subseteq \mathbb{R}^{32 \times 12}$, corresponds to a history of the last 32 force and torque readings from both arms (concatenated), while the robot state space, $\mathcal{S} \subseteq \mathbb{R}^{14}$, represents the end-effector positions and orientations (expressed as quaternions) for both arms (concatenated). Our action space, $\mathcal{A} = [0, 1]^3$,

consists of end-effector position deltas relative to the current pose.

Policy Learning: The goal is to learn a policy $\pi : \mathcal{O} \rightarrow \mathcal{A}$ that maps observations to actions, enabling task completion. In the imitation learning setting, an expert policy π^* is provided, where $a^* = \pi^*(o)$ represents the optimal action for an observation $o \in \mathcal{O}$. Our objective is to learn a policy π that closely resembles the behavior of π^* . There are several approaches to learning such a policy from demonstrations, with the simplest being *behavior cloning*. In behavior cloning, the expert provides a dataset of N demonstration trajectories $\mathcal{D} = \{ \{ (o_i, a_i^*) \}_{i=1}^{n_j} \}_{j=1}^N$, where n_j is the horizon for demonstration j . The policy π is then trained to replicate the expert actions from π^* for the corresponding observations using supervised learning. We train our observation encoder and policy network (shown in Figure 3) end-to-end using an L_2 loss between expert and predicted actions.

B. Data Collection with Human Experts

We collect a dataset of 50 human demonstrations in our simulation environment, built using the Robosuite framework [20] with MuJoCo [7] as the simulation engine. All demonstrations are performed in the canonical environment setup described in Section III-C. A human expert teleoperates the robot’s moving arm via keyboard inputs, with actions recorded as the difference between the end-effector positions in consecutive frames. The simulation automatically terminates and records the demonstration upon detecting a successful completion.

C. Multisensory Data Augmentation

A common technique to enhance a model’s robustness without requiring additional human effort in data collection is data augmentation, which involves transforming input data while preserving the original labels. This approach is most commonly used with image inputs, where transformations such as cropping, flipping, and color adjustments are applied to help the model learn invariance to these changes [3], [21], [22]. Image augmentation can also be performed at the semantic level using generative models [23]. However, applying this type of augmentation to contact-rich tasks poses challenges, as these tasks involve *physical* variations (e.g., object size, shape), which may introduce non-independent perturbations across the multisensory input that cannot be captured through conventional offline augmentation.

To address this, we employ an *online* data augmentation technique by replaying human-generated trajectories on task instances with identical initial offsets but with a subset of

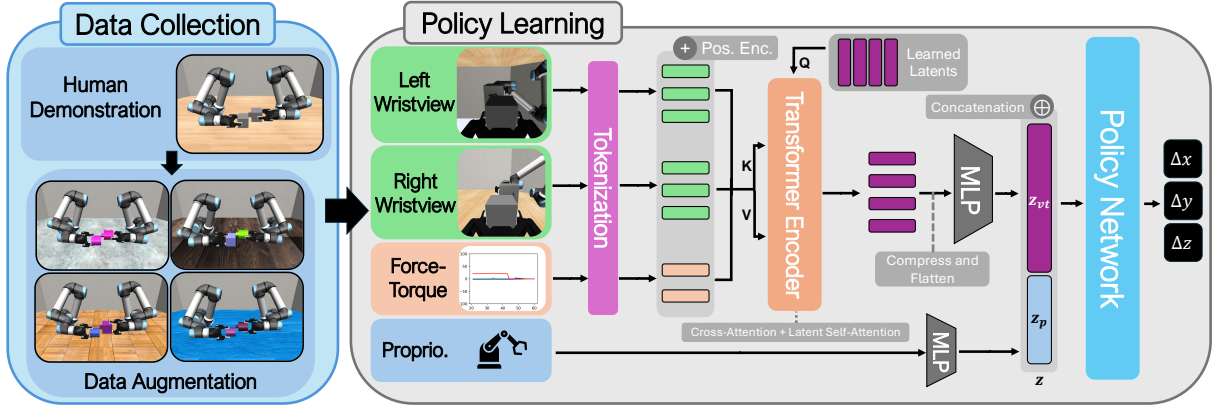


Fig. 3: An overview of our data collection and policy learning framework. We use BC-MLP [17] with a multilayer perceptron policy network to output actions. Image and force-torque observations are encoded with a visuotactile transformer [2] that includes a cross-attention step with a set of learned latent vectors (similar to Perceiver IO [18], [19]). More details on our network architecture can be found in our supplementary material and website.

task variations applied. Given the previously-defined dataset of expert demonstration trajectories \mathcal{D} , the set of all possible task variations \mathcal{V} , and a function $f_{\mathcal{K}} : \mathcal{O} \rightarrow \mathcal{O}$ that returns an input observation with a subset $\mathcal{K} \subseteq \mathcal{V}$ of task variations applied, our online augmentation process takes an expert demonstration $d_j = \{(o_i, a_i^*)\}_{i=1}^{n_j} \in \mathcal{D}$ and outputs a set of new demonstrations $\Omega_{d_j} = \{ \{ (f_{\mathcal{K}}^t(o_i), a_i^*) \}_{i=1}^{n_j} \}_{t=1}^T$, where T is the number of augmentations per expert demonstration. The indexed functions $f_{\mathcal{K}}^1, \dots, f_{\mathcal{K}}^T$ indicate that although each application of task variations \mathcal{K} is different between each generated demonstration in Ω_{d_j} , the specific application of \mathcal{K} is consistent for each observation in a given augmented demonstration. After the augmentation process, we construct a new dataset $\hat{\mathcal{D}} = \mathcal{D} \cup \left(\bigcup_{n=1}^N \Omega_{d_n} \right)$ that can be used for training.

V. EXPERIMENTAL SETUP

We conduct experiments to evaluate the robustness of our model with respect to each of the 6 implemented task variations (see Section III-C), as well as a combination of all variations (denoted as *All Variations*).

A. Training and Evaluation Details

In all experiments, we train the models for 100 epochs and perform 50 rollouts on the same task variations used in the training dataset. The model checkpoint that achieves the highest success rate in these rollouts during training is selected for evaluation. This training process is conducted over 6 random seeds per model, and the performance is averaged across all seeds during evaluation. A rollout is considered successful if it results in a successful insertion, and it is deemed failed if the maximum horizon is exceeded without insertion. Additionally, a rollout fails if the force-torque measurement surpasses a predefined threshold, to prevent unsafe behavior that could damage the robot arms or objects.

B. Evaluation on Unseen Task Variation Instances

To ensure rigorous evaluation, we explicitly separate task variation instances encountered during training from those

used for evaluation within each variation category. For instance, when training with *Grasp Pose* variations, we include demonstrations involving x-axis translation and z-axis translation and rotation, while reserving y-axis rotation for evaluation. This approach guarantees that the model encounters unseen variations during evaluation, enabling us to assess its generalization to out-of-distribution inputs across all variation categories. A detailed overview of training versus evaluation instances for each variation category is provided in Table I.

Task Variation	Train Instances	Eval Instances
<i>Grasp Pose</i> [16]	XT, ZT, ZR	XT, ZT, ZR, YR
<i>Peg/Hole Shape</i>	key, circle, cross	arrow, u, pentagon, line, hexagon, diamond
<i>Object Body Shape</i>	Peg/Hole Objects: cube, cylinder	Hole Object: cube, cylinder, octagonal prism, Peg Object: thin cube, cylinder, and octagonal prism
<i>Scene Appearance</i>	6 floor textures, object color	14 unseen floor textures, object color, lighting

TABLE I: Instances for task variations during training (if included the training set) and evaluation. Task variations not in this table are the same both in training and evaluation.

VI. EXPERIMENTS AND RESULTS

In this section, we address a series of questions related to generalization through experimental evaluations.

A. Which task variations are most difficult to generalize to?

In determining the difficulty of generalizing to each of our task variations, we train a model exclusively on human-collected demonstrations without any task variations applied and report the success rate for each task variation during evaluation. These results can be found in Figure 4.

Takeaways: We observe that *Grasp Pose* variations the hardest challenge to generalize to out of all of the individual

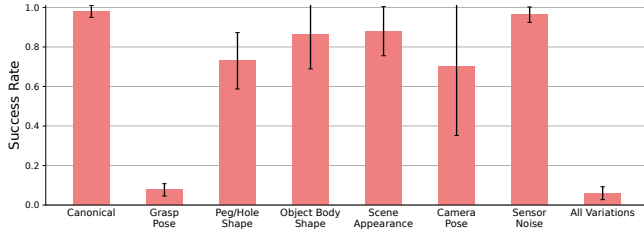


Fig. 4: Success rates on each task variation for a model trained exclusively on non-augmented human demonstration data. Error bars represent one standard deviation from the mean. The model suffers the largest success rate drop compared to the canonical environment when evaluated on *Grasp Pose* variations, and subsequently does poorly when evaluated on *All Variations*.

task variations, as we see a drop from a mean success rate of **0.987** on *Canonical* rollouts with no task variations to **0.087** when *Grasp Pose* variations are applied. We hypothesize that the large negative impact on performance comes from the significant perturbation that grasp variations apply to all sensing modalities, unlike other variations such as *Scene Appearance* and *Sensor Noise* which only target specific modalities and thus have a smaller negative impact for the overall model.

B. Which task variations included in the training set produce the largest impact on robustness?

To evaluate the effect of introducing task variations to the training dataset, we evaluate models trained on datasets augmented with different subsets of our task variations. These datasets contain the original collected human demonstrations as well as 6 augmentations per demonstration, with each augmentation containing a composition of all the task variations included in the dataset (which we refer to as the “training set variations” for that specific dataset). We evaluate these models both on instances of their training set variations that were unseen during training (as discussed in Section V-B) as well as all variations not included in the training set (which we refer to as the “evaluation set variations” for that specific dataset). We report % success rate change from the canonical environment success rate averaged over 6 seeds for each variation in Figure 5, defined as

$$\% \text{ success rate change} = \frac{\text{task var. success} - \text{canon. success}}{\text{canon. success}}$$

Takeaways: We observe that the additions of peg and hole shape, object body shape, and grasp variations (considered the *Base* variations for this task) greatly reduce the generalization gap on unseen instances of these variations during evaluation. Curiously, we also observe a reduced generalization gap for a dataset with the *Base* training set variations on the evaluation set variations of *Scene Appearance* and *Camera Angle*, even though these variations had not been explicitly included in the dataset. This may be due to the similarity between the effects of applying grasp variations and perturbing the camera angle, as both alter the view of the object held by the gripper and the opposing object. Additionally, the resulting visual variations may have

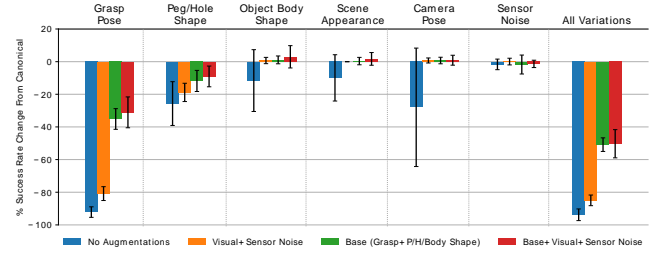


Fig. 5: % success rate changes on each task variation for models trained on different subsets of task variations. Error bars represent one standard deviation from the mean. The addition of grasp variations to the training set greatly improves generalization to unseen grasp variations, while visual variations and sensor noise do not have any significant effect on generalization ability on physical task variations.

contributed to improving the model’s robustness to changes in scene appearance. Explicitly adding both visual variations (*Scene Appearance* and *Camera Angle*) and *Sensor Noise* to the training set does not further enhance generalization to their respective variations during evaluation.

C. Can increasing the number of augmentations per demonstration improve robustness?

Building off of our investigation into determining the ideal training set variations, we also seek to analyze the effect of adding more augmentations per demonstration involving these variations. Aligning with the previous experiment, we choose *Grasp Pose*, *Peg/Hole Shape*, and *Object Body Shape* as our training set variations, and train models on datasets with different numbers of augmentations per human demonstration. Success rates on each task variation are reported in Figure 6.

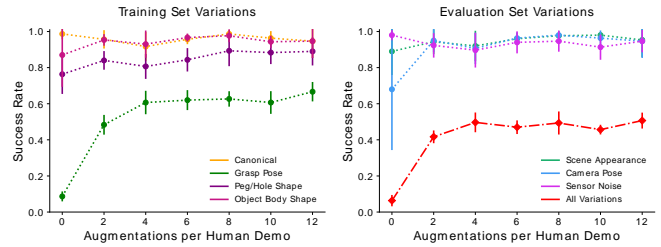


Fig. 6: Success rates on each task variation for models trained on a base set of training variations with different number of augmentations for each human demonstration. *All Variations* represents a composition of both training set and evaluation set variations. Error bars represent one standard deviation from the mean. Success rate on *Grasp Pose* variations increases the most with an increasing number of augmentations, while the other task variations maintain stable success rates.

Takeaways: The most significant improvement in success rate as the number of augmentations increases seems to be the performance on *Grasp Pose* evaluations, with a more subtle upward trend in the other training set variations. Since the task variations of *Peg/Hole Shape* and *Object Body Shape* are discrete variations with a small subset of all possible shapes being included in the training set, they would benefit less from having more augmentations as the dataset would start to contain redundant instances of these variations. *Grasp*

Pose variations, on the other hand, are continuous and so would benefit more from a larger sample of grasps. For the evaluation set variations (aside from *All Variations*), the success rate remains stable, suggesting that the model is not overfitting to the training set variations even when the dataset has more samples biased towards those perturbations.

D. How much does each sensory modality contribute to model robustness?

In an effort to investigate the significance of each of the modalities in our system—vision (wristview cameras), touch (force-torque), and proprioception—we conduct an ablation study with models that have one or more input modalities missing. We evaluate each model when trained on a dataset with no variations (i.e. no augmentations) and a dataset with 6 augmentations per demonstration on a training variation set of *Grasp Pose*, *Peg/Hole Shape*, and *Object Body Shape* to analyze how each modality combination reacts when task variations are introduced during training. Figure 7 shows reported % success rate change from the canonical environment success rate averaged over 6 seeds for each variation.

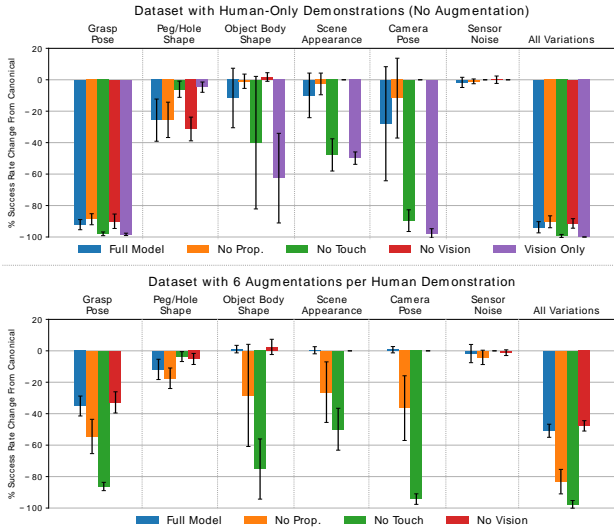


Fig. 7: % success rate changes on each task variation for models with different modality input combinations trained on no task variations (top) or a subset of task variations (bottom). The *Vision Only* model is omitted from the bottom plot due to training instability. Error bars represent one standard deviation from the mean. The removal of force-torque input sees the largest % success rate drop for many of the task variations out of each of the individual modalities, while the removal of vision has little impact on % success rate change compared to the full model.

Takeaways: We observe that out of the individual modalities, *No Touch* has the highest success rate drop for many of the variations (*Peg/Hole Shape* and *Sensor Noise* being the only exceptions) for both human-only and augmented demonstrations. On the other hand, *No Vision* has comparable (or sometimes even improved) % success rate changes to *Full Model*, suggesting its reduced significance in our overall framework compared to the other modalities. Since our task begins immediately in a contact state that is maintained

throughout a majority of the task’s duration, it follows that force-torque provides the most valuable information about the task state. Proprioception may also give important task state information (as evidenced in the % success rate change for the *No Prop.* model), as the position of the two end-effectors relative to each other is highly correlated to the position of the peg and hole relative to each other, which is essential knowledge in completing the insertion task. Thus, visual observations provide the least relevant information for our task while still being susceptible to many of the task variations. However, visual input may still be essential in task contexts outside of the one studied here, especially in situations with little to no force-torque feedback (such as aligning the peg and hole objects to be in the same orientation before contact as was studied in our previous work [16]).

E. Additional Experiments

We perform a set of additional experiments to gain more insight into our system, the full results of which can be found in our supplementary material and website.

Attention Visualization: We plot attention weights in the cross-attention step of the visuotactile encoder averaged over the learned latent vectors and find that tokens from the tactile input take up a much larger proportion of attention than the visual tokens throughout the task, despite there being twice as many visual tokens as tactile ones. This provides further evidence of the importance of tactile over visual information first discussed in Section VI-D.

Real World Experiments: We construct a real-world setup of our insertion task and conduct a smaller-scale robustness experiment to compare with our results gathered in simulation.

VII. CONCLUSION

We present a pipeline for data collection, augmentation, policy training, and evaluation to learn robust policies for an object assembly task across diverse observation-level task variations. Our experiments reveal that grasp variations pose the greatest challenge for generalization, and incorporating them through data augmentation significantly improves performance on unseen variations. Additionally, we demonstrate that force-torque input is critical for robustness to task variations, while the removal of RGB input has minimal impact.

While we have demonstrated the ability of our system to learn the underlying task, we acknowledge that the behavior cloning setup used is highly susceptible to covariate shift and cannot recover from erroneous actions. We plan to extend our generalization studies using more advanced imitation learning frameworks, such as Diffusion Policy [24] and ACT [25], and compare their performance with our BC-MLP setup. Moreover, the constrained task initialization and action space in our setup highlight the need to explore more complex, longer-horizon tasks with broader action spaces, and to assess how observation-level task variations affect policies in these contexts.

REFERENCES

- [1] M. A. Lee, Y. Zhu, K. Srinivasan, P. Shah, S. Savarese, L. Fei-Fei, A. Garg, and J. Bohg, “Making sense of vision and touch: Self-supervised learning of multimodal representations for contact-rich tasks,” in *2019 International conference on robotics and automation (ICRA)*. IEEE, 2019, pp. 8943–8950.
- [2] Y. Chen, M. Van der Merwe, A. Sipos, and N. Fazeli, “Visuo-tactile transformers for manipulation,” in *Conference on Robot Learning*. PMLR, 2023, pp. 2026–2040.
- [3] O. Spector and D. Di Castro, “Insertionnet-a scalable solution for insertion,” *IEEE Robotics and Automation Letters*, vol. 6, no. 3, pp. 5509–5516, 2021.
- [4] O. Spector, V. Tchuiev, and D. Di Castro, “Insertionnet 2.0: Minimal contact multi-step insertion using multimodal multiview sensory input,” in *2022 International Conference on Robotics and Automation (ICRA)*. IEEE, 2022, pp. 6330–6336.
- [5] A. Xie, L. Lee, T. Xiao, and C. Finn, “Decomposing the generalization gap in imitation learning for visual robotic manipulation,” in *2024 IEEE International Conference on Robotics and Automation (ICRA)*. IEEE, 2024, pp. 3153–3160.
- [6] W. Pumacay, I. Singh, J. Duan, R. Krishna, J. Thomason, and D. Fox, “The colosseum: A benchmark for evaluating generalization for robotic manipulation,” *arXiv preprint arXiv:2402.08191*, 2024.
- [7] E. Todorov, T. Erez, and Y. Tassa, “Mujoco: A physics engine for model-based control,” in *2012 IEEE/RSJ International Conference on Intelligent Robots and Systems*, 2012, pp. 5026–5033.
- [8] M. A. Lee, M. Tan, Y. Zhu, and J. Bohg, “Detect, reject, correct: Crossmodal compensation of corrupted sensors,” in *2021 IEEE international conference on robotics and automation (ICRA)*. IEEE, 2021, pp. 909–916.
- [9] A. Vaswani, “Attention is all you need,” *Advances in Neural Information Processing Systems*, 2017.
- [10] C. Kohler, A. S. Srikanth, E. Arora, and R. Platt, “Symmetric models for visual force policy learning,” in *2024 IEEE International Conference on Robotics and Automation (ICRA)*. IEEE, 2024, pp. 3101–3107.
- [11] E. Xing, A. Gupta, S. Powers, and V. Dean, “Kitchenshift: Evaluating zero-shot generalization of imitation-based policy learning under domain shifts,” in *NeurIPS 2021 Workshop on Distribution Shifts: Connecting Methods and Applications*, 2021. [Online]. Available: <https://openreview.net/forum?id=DdglKo8hBq0>
- [12] J. Gao, A. Xie, T. Xiao, C. Finn, and D. Sadigh, “Efficient data collection for robotic manipulation via compositional generalization,” *arXiv preprint arXiv:2403.05110*, 2024.
- [13] A. Mandlekar, S. Nasiriany, B. Wen, I. Akinola, Y. Narang, L. Fan, Y. Zhu, and D. Fox, “Mimicgen: A data generation system for scalable robot learning using human demonstrations,” in *Conference on Robot Learning*. PMLR, 2023, pp. 1820–1864.
- [14] M. Jia, D. Wang, G. Su, D. Klee, X. Zhu, R. Walters, and R. Platt, “Seil: simulation-augmented equivariant imitation learning,” in *2023 IEEE International Conference on Robotics and Automation (ICRA)*. IEEE, 2023, pp. 1845–1851.
- [15] L. Ankile, A. Simeonov, I. Shenfeld, and P. Agrawal, “Juicer: Data-efficient imitation learning for robotic assembly,” *arXiv preprint arXiv:2404.03729*, 2024.
- [16] C. Ku, C. Winge, R. Diaz, W. Yuan, and K. Desingh, “Evaluating robustness of visual representations for object assembly task requiring spatio-geometrical reasoning,” in *2024 IEEE International Conference on Robotics and Automation (ICRA)*. IEEE, 2024, pp. 831–837.
- [17] A. Mandlekar, D. Xu, J. Wong, S. Nasiriany, C. Wang, R. Kulkarni, L. Fei-Fei, S. Savarese, Y. Zhu, and R. Martín-Martín, “What matters in learning from offline human demonstrations for robot manipulation,” in *Conference on Robot Learning*. PMLR, 2022, pp. 1678–1690.
- [18] A. Jaegle, F. Gimeno, A. Brock, O. Vinyals, A. Zisserman, and J. Carreira, “Perceiver: General perception with iterative attention,” in *International conference on machine learning*. PMLR, 2021, pp. 4651–4664.
- [19] A. Jaegle, S. Borgeaud, J.-B. Alayrac, C. Doersch, C. Ionescu, D. Ding, S. Koppula, D. Zoran, A. Brock, E. Shelhamer *et al.*, “Perceiver io: A general architecture for structured inputs & outputs,” in *International Conference on Learning Representations*, 2022.
- [20] Y. Zhu, J. Wong, A. Mandlekar, R. Martín-Martín, A. Joshi, S. Nasiriany, and Y. Zhu, “robosuite: A modular simulation framework and benchmark for robot learning,” *arXiv preprint arXiv:2009.12293*, 2020.
- [21] L. Perez, “The effectiveness of data augmentation in image classification using deep learning,” *arXiv preprint arXiv:1712.04621*, 2017.
- [22] X. Zhu, D. Wang, O. Biza, G. Su, R. Walters, and R. Platt, “Sample efficient grasp learning using equivariant models,” in *Robotics: Science and Systems*, 2022.
- [23] Z. Chen, S. Kiami, A. Gupta, and V. Kumar, “Genaug: Retargeting behaviors to unseen situations via generative augmentation,” *arXiv preprint arXiv:2302.06671*, 2023.
- [24] C. Chi, Z. Xu, S. Feng, E. Cousineau, Y. Du, B. Burchfiel, R. Tedrake, and S. Song, “Diffusion policy: Visuomotor policy learning via action diffusion,” *The International Journal of Robotics Research*, 2024.
- [25] T. Z. Zhao, V. Kumar, S. Levine, and C. Finn, “Learning fine-grained bimanual manipulation with low-cost hardware,” *arXiv preprint arXiv:2304.13705*, 2023.